

Joint Time and Frequency Synchronization for Distributed Beamforming in Decode-and-Forward Relaying Systems Using Importance Sampling

Souheib Ben Amor*, Faouzi Bellili*, Sofiène Affes*, Usa Vilaipornasawai†, Liqing Zhang†, and Peiyong Zhu†

*INRS-EMT, Université du Québec, Montréal, QC, Canada, Emails: {souheib.ben.amor, bellili, affes}@emt.inrs.ca

†Huawei Technologies Canada Co. Ltd., Kanata, ON, Canada, Emails: {usa.vilaipornasawai, liqing.zhang, peiyong.zhu}@huawei.com

Abstract—In this paper, we tackle the problem of joint time and frequency synchronization for decode-and-forward (DF) systems. We devise a new maximum likelihood (ML) algorithm for the joint estimation of these synchronization parameters based on the importance sampling (IS) technique. Unlike the traditional iterative estimation techniques, the proposed IS-based ML approach enjoys guaranteed global optimality. Moreover, it transforms the original multi-dimensional optimization problem into multiple two-dimensional ones, thereby entailing low computational burden. Simulation results show the advantage of the IS-based ML estimator over state-of-the-art estimation techniques.

I. INTRODUCTION

Cooperative communication is an effective solution to generate spatial diversity using relaying nodes. In fact, the main idea is to retransmit multiple copies of the same signal by different relays. In the course of building a robust cooperative communication protocol, several issues must be addressed such as cooperation assignment and transmit requirements on the nodes. To address these issues and establish an organized communication between the different nodes, clock synchronization is required for different critical reasons. In fact, it is crucial to perform data fusion in all distributed networks where the goal is to process and integrate the data in the best possible way. Besides, clock synchronization is needed in distributed signal processing applications that take “time information” into account. Finally, scheduling protocols such as time division multiple access (TDMA) cannot be performed if the different nodes do not speak the same time language.

One of the main issues related to clock synchronization in cooperative communications is time and frequency synchronization of various cooperating nodes. This is essential if the relays need to perform distributed beamforming at the transmitter (DBT). The latter stands at the forefront of scientific research on cooperative communication as it increases communication range, energy efficiency, and achievable data rates. Indeed, the ultimate goal of DBT is to ensure that multiple copies of a signal originating from different relay nodes i) arrive simultaneously and ii) combine constructively at the destination. Many existing works have focused on objective i) by estimating and then pre-compensating the multiple timing offsets (MTOs) while assuming perfect carrier synchronization [1-4]. Many other works focused on objective ii) by estimating the multiple frequency offsets (MFOs) while assuming perfect time synchronization [5-9]. It was only recently,

though, that the joint estimation of the MTOs and CFOs was investigated. In this context, [10] proposed joint ML estimation techniques for the MTOs, MFOs, and channel gains. By exploiting the cyclic prefix of orthogonal frequency-division multiple-access (OFDMA) systems, [11-14] also tackled the problem of joint channel estimation and time-frequency synchronization. However, depending on the number of subcarriers used, the frequency acquisition range of the proposed algorithms is very limited. More recently, the problem of estimating jointly the MTOs, MFOs, and channel gains was addressed in [15] for the DF relaying scheme. However, the ML solution proposed there is iterative in nature and, as such, does not guarantee convergence to the global maximum of the likelihood function.

In this paper, we propose a new non-iterative ML technique that always achieves the global maximum of the CLF. We also avoid the high computation complexity of the brute grid search approach by resorting to the IS technique. By doing so, we show that the multi-dimensional maximization problem can be transformed into multiple 2-D optimization ones.

The rest of this paper is organized as follows. In Section II, we introduce the system model. The maximization of the compressed likelihood function (CLF) is presented in Section III. We also provide the required details about the maximization of the CLF in Section IV. In Section V, we assess by computer simulations the performance of the new algorithm. Finally, we draw out some concluding remarks in section VI.

We adopt the following common notations. Bold-font small letters and bold-font capital letters denote vectors and matrices, respectively. The conjugate and Hermitian are represented by $\{\cdot\}^T$ and $\{\cdot\}^H$, respectively. The Euclidean norm of any vector is denoted as $\|\cdot\|$ and \mathbf{I}_N denotes the $(N \times N)$ identity matrix. We denote by $\det\{\cdot\}$ the determinant of any square matrix. The superscript $\{\cdot\}^*$ and $|\cdot|$ return the conjugate and modulus of any complex number, respectively. Finally, $\mathbb{E}\{\cdot\}$ stands for the statistical expectation, j is the pure complex number that verifies $j^2 = -1$, and the notation \triangleq is used for definitions.

II. SYSTEM MODEL

Consider a DF relaying network with one source node, \mathbb{S} , a single destination node, \mathbb{D} , and K relays, R_1, R_2, \dots, R_K . We assume that the links between the source and the relays and those between the relays and the destination are characterized by quasi-static and frequency flat-fading channels. We refer to the channel gain between the source and k^{th} relay by $\bar{\gamma}_k$. Similarly, $\bar{\eta}_k$ denotes the channel gain between the k^{th} relay and

Work supported by the NSERC/Huawei Canada/TELUS CRD Grant on 5G-WAVES (WAV Enabling Schemes), the DG and CREATE PERSWADE <www.create-perswade.ca> Programs of NSERC, and a Discovery Accelerator Supplement Award from NSERC.

the destination node. Each channel is modelled by a zero-mean complex Gaussian random variable, i.e., $\bar{\gamma}_k \sim \mathcal{CN}(0, \sigma_\gamma^2)$ and $\bar{\eta}_k \sim \mathcal{CN}(0, \sigma_\eta^2)$. The source begins by broadcasting a training sequence, $\mathbf{t}^{[s]} \triangleq [t^{[s]}(0), t^{[s]}(1), \dots, t^{[s]}(L-1)]^T$ of L symbols to the K relays. The continuous-time received signal at the k^{th} relay is then given by:

$$r_k(t) = \bar{\gamma}_k \sum_{n=0}^{L-1} t^{[s]}(n) g\left(t - nT - \tau_k^{[sr]}\right) e^{j2\pi\bar{\nu}_k^{[sr]}t} + u_k(t), \quad (1)$$

where $u_k(t)$ is the white additive noise at the k^{th} node, $g(t)$ denotes the square-root raised-cosine function (SRRC) and T refers to the symbol duration. The timing and carrier frequency offsets between the source and the k^{th} relay are denoted by $\tau_k^{[sr]}$ and $\bar{\nu}_k^{[sr]}$, respectively. Once the signal received, each relay can decode the upcoming data using conventional SISO synchronization techniques such as in [16]. In the next step, all the relays start by transmitting their own training sequences, $\mathbf{t}_k^{[r]} \triangleq [t_k^{[r]}(0), t_k^{[r]}(1), \dots, t_k^{[r]}(L-1)]^T$ before forwarding the useful data to the destination node. The signal at the destination is up-sampled with a factor $Q = T/T_s$, leading to the following received samples for $i = 0, 1, \dots, QL - 1$:

$$x(i) = \sum_{k=1}^K \bar{\eta}_k e^{j2\pi\bar{\nu}_k^{[rd]}i/Q} \sum_{n=0}^L t_k^{[r]}(n) g\left(iT_s - nT - \bar{\tau}_k^{[rd]}\right) + n(i), \quad (2)$$

in which T_s is the sampling period and $n(i) \sim \mathcal{CN}(0, \sigma^2)$ is the white additive noise at the destination. The synchronization parameters $\bar{\tau}_k^{[rd]}$ and $\bar{\nu}_k^{[rd]}$ refer to the timing and carrier frequency offsets between the k^{th} relay and the destination node, respectively. The vector form of (2) can be written as follows:

$$\mathbf{x} = \left[\Lambda\left(\bar{\nu}_1^{[rd]}\right) \mathbf{G}\left(\bar{\tau}_1^{[rd]}\right) \mathbf{t}_1^{[r]}, \dots, \Lambda\left(\bar{\nu}_K^{[rd]}\right) \mathbf{G}\left(\bar{\tau}_K^{[rd]}\right) \mathbf{t}_K^{[r]} \right] \bar{\boldsymbol{\eta}} + \mathbf{n}, \quad (3)$$

with $\mathbf{x} \triangleq [x(0), x(1), \dots, x(QL-1)]^T$ and $\bar{\boldsymbol{\eta}} \triangleq [\bar{\eta}_1, \dots, \bar{\eta}_K]^T$. The noise components, $\{n(i)\}_{i=0}^{QL-1}$, are gathered in $\mathbf{n} \triangleq [n(0), n(1), \dots, n(QL-1)]^T$. The two matrices, i.e., $\mathbf{G}(\tau)$ and $\Lambda(\nu)$, involved in (3) are expressed as follows:

$$\mathbf{G}(\tau) \triangleq \begin{pmatrix} g(0-T-\tau) & \dots & g(0-LT-\tau) \\ g(T_s-T-\tau) & \dots & g(T_s-LT-\tau) \\ \vdots & \vdots & \vdots \\ g((QL-1)T_s-T-\tau) & \dots & g((QL-1)T_s-LT-\tau) \end{pmatrix}, \quad (4)$$

$$\Lambda(\nu) \triangleq \text{diag}\left\{ \left[1, e^{j2\pi\nu}, \dots, e^{j2\pi\nu(QL-1)/Q} \right] \right\}. \quad (5)$$

For the sake of clarity, we adopt the following notations:

$$\begin{aligned} \Psi(\nu, \tau) &\triangleq \Lambda(\nu) \mathbf{G}(\tau), \\ \mathbf{D}(\boldsymbol{\nu}, \boldsymbol{\tau}) &\triangleq \left[\Psi(\nu_1, \tau_1) \mathbf{t}_1^{[r]} \quad \Psi(\nu_2, \tau_2) \mathbf{t}_2^{[r]} \quad \dots \quad \Psi(\nu_K, \tau_K) \mathbf{t}_K^{[r]} \right]. \end{aligned}$$

We define also the following parameter vectors: $\bar{\boldsymbol{\nu}} \triangleq [\bar{\nu}_1, \bar{\nu}_2, \dots, \bar{\nu}_K]^T$ and $\bar{\boldsymbol{\tau}} \triangleq [\bar{\tau}_1, \bar{\tau}_2, \dots, \bar{\tau}_K]^T$. From now on, we use $\bar{\boldsymbol{\nu}}$ (resp. $\bar{\boldsymbol{\tau}}$) to refer to $\bar{\boldsymbol{\nu}}^{[rd]}$ (resp. $\bar{\boldsymbol{\tau}}^{[rd]}$). With these common notations, it is clear from (3) that the model for the DF scheme is given by:

$$\mathbf{x} = \mathbf{D}(\bar{\boldsymbol{\nu}}, \bar{\boldsymbol{\tau}}) \bar{\boldsymbol{\eta}} + \mathbf{n}. \quad (6)$$

III. JOINT CFOs AND MTOs ESTIMATION

In this section, we derive a new technique that builds upon the powerful theorem of Pincus [17] to fetch the global maximum of the likelihood function. Based on our system model, the CLF which depends only on $\bar{\boldsymbol{\nu}}$ and $\bar{\boldsymbol{\tau}}$ is given by [15]:

$$\mathcal{L}_c(\boldsymbol{\nu}, \boldsymbol{\tau}) = \mathbf{x}^H \mathbf{D}(\mathbf{D}^H \mathbf{D})^{-1} \mathbf{D}^H \mathbf{x}, \quad (7)$$

and the joint ML estimates of $\boldsymbol{\nu}$ and $\boldsymbol{\tau}$ are hence obtained as the solution to the following optimization problem:

$$[\hat{\boldsymbol{\nu}}_{\text{MLE}}, \hat{\boldsymbol{\tau}}_{\text{MLE}}] = \underset{\boldsymbol{\nu}, \boldsymbol{\tau}}{\text{argmax}} \mathcal{L}_c(\boldsymbol{\nu}, \boldsymbol{\tau}). \quad (8)$$

It is clear that finding the global maximum of the CLF in (8) by a grid search is computationally intractable since the maximization is performed over $2K$ unknown parameters. Iterative solutions as in [15] can be envisaged here without guarantees, however, for global convergence. To sidestep this problem, we opt here for a global optimization technique that relies on the Pincus theorem introduced in [17]. The latter provides a closed-form solution to any $2K$ -dimensional optimization problem pending some mild assumptions on the underlying objective function. In fact, for any function $f(\boldsymbol{\theta})$ that has a global maximum, where $\boldsymbol{\theta} = [\theta_1, \dots, \theta_{2K}]$, Pincus' theorem states that the global maximum of $f(\cdot)$ is obtained as:

$$\hat{\theta}_k = \frac{\int \dots \int \theta_k e^{\rho_0 f(\boldsymbol{\theta})} d\boldsymbol{\theta}}{\int \dots \int e^{\rho_0 f(\boldsymbol{\theta})} d\boldsymbol{\theta}}, \quad \text{for } k = 1, \dots, 2K, \quad (9)$$

for some sufficiently high value ρ_0 . In our case, the result in (9) can be applied to find the global maximum of $f(\boldsymbol{\theta}) \triangleq \mathcal{L}_c(\boldsymbol{\nu}, \boldsymbol{\tau})$ by setting $\boldsymbol{\theta}$ equal to $[\boldsymbol{\nu}, \boldsymbol{\tau}]$. Therefore, we obtain the following estimates:

$$\hat{\tau}_{k, \text{MLE}} = \int \dots \int \tau_k \bar{\mathcal{L}}_c(\boldsymbol{\nu}, \boldsymbol{\tau}) d\boldsymbol{\nu} d\boldsymbol{\tau}, \quad k = 1, 2, \dots, K \quad (10)$$

$$\hat{\nu}_{k, \text{MLE}} = \int \dots \int \nu_k \bar{\mathcal{L}}_c(\boldsymbol{\nu}, \boldsymbol{\tau}) d\boldsymbol{\nu} d\boldsymbol{\tau}, \quad k = 1, 2, \dots, K \quad (11)$$

where $\bar{\mathcal{L}}_c(\boldsymbol{\nu}, \boldsymbol{\tau})$ is the *normalized* CLF defined as:

$$\bar{\mathcal{L}}_c(\boldsymbol{\nu}, \boldsymbol{\tau}) \triangleq \frac{e^{\rho_0 \mathcal{L}_c(\boldsymbol{\nu}, \boldsymbol{\tau})}}{\int \dots \int e^{\rho_0 \mathcal{L}_c(\boldsymbol{\nu}, \boldsymbol{\tau})} d\boldsymbol{\nu} d\boldsymbol{\tau}}. \quad (12)$$

The design parameter ρ_0 involved in (12) has a crucial role in the estimation process. In fact, if ρ_0 tends to infinity, the *normalized* CLF becomes a Dirac-delta function located around the global maximum. In addition, the *normalized* CLF in (12) is a nonnegative function and integrates to one. As a consequence, it has the main properties of a pdf. As such, the estimates in (10) and (11) can be seen as statistical expectations expressed as follows:

$$\hat{\tau}_{k, \text{MLE}} = \mathbb{E}_{\boldsymbol{\nu}, \boldsymbol{\tau}} \{\tau_k\} \quad \text{and} \quad \hat{\nu}_{k, \text{MLE}} = \mathbb{E}_{\boldsymbol{\nu}, \boldsymbol{\tau}} \{\nu_k\}, \quad (13)$$

with $\boldsymbol{\tau}$ and $\boldsymbol{\nu}$ being distributed according to $\bar{\mathcal{L}}_c(\boldsymbol{\nu}, \boldsymbol{\tau})$. To find the expectations in (13), however, one needs to generate R realizations, $\{\boldsymbol{\tau}^{(r)}\}_{r=1}^R$ and $\{\boldsymbol{\nu}^{(r)}\}_{r=1}^R$, with respect to $\bar{\mathcal{L}}_c(\boldsymbol{\tau}, \boldsymbol{\nu})$. These realizations are used to obtain the following sample means estimates:

$$\hat{\tau}_{k, \text{MLE}} = \frac{1}{R} \sum_{r=1}^R \tau_k^{(r)} \quad \text{and} \quad \hat{\nu}_{k, \text{MLE}} = \frac{1}{R} \sum_{r=1}^R \nu_k^{(r)}. \quad (14)$$

It is worth noting that the approximated estimates in (14) become closer to the global maximum of the CLF as the number of generated realizations increases. In the next section, we propose a simple approach based on the IS concept in order to generate the required realizations with reduced complexity.

IV. IS-BASED ML ESTIMATOR

A. Importance Sampling Concept

The main technical issue encountered in the previous section is related to the process of generating the required realizations. Indeed, the *normalized CLF* $\bar{\mathcal{L}}_c(\boldsymbol{\nu}, \boldsymbol{\tau})$ is extremely non-linear. Yet, this problem can be easily circumvented owing to the IS concept where, instead of using the true pseudo-pdf $\bar{\mathcal{L}}_c(\boldsymbol{\nu}, \boldsymbol{\tau})$, one relies on another pseudo-function to generate the required realizations. It follows that the estimates in (10) and (11) can be rewritten as follows at the k^{th} relay:

$$\hat{\tau}_{k,\text{MLE}} = \int \cdots \int \tau_k \frac{\bar{\mathcal{L}}_c(\boldsymbol{\nu}, \boldsymbol{\tau})}{\bar{\mathcal{G}}(\boldsymbol{\nu}, \boldsymbol{\tau})} \bar{\mathcal{G}}(\boldsymbol{\nu}, \boldsymbol{\tau}) d\boldsymbol{\nu} d\boldsymbol{\tau}, \quad (15)$$

$$\hat{\nu}_{k,\text{MLE}} = \int \cdots \int \nu_k \frac{\bar{\mathcal{L}}_c(\boldsymbol{\nu}, \boldsymbol{\tau})}{\bar{\mathcal{G}}(\boldsymbol{\nu}, \boldsymbol{\tau})} \bar{\mathcal{G}}(\boldsymbol{\nu}, \boldsymbol{\tau}) d\boldsymbol{\nu} d\boldsymbol{\tau}, \quad (16)$$

with $\bar{\mathcal{G}}(\boldsymbol{\nu}, \boldsymbol{\tau})$ being the importance function that needs to be designed as close as possible to the original pseudo-pdf while allowing at the same time the easy generation of the required realizations. The ML estimates (MLEs) could then be interpreted as expected values of the new transformed realizations as follows:

$$\hat{\tau}_{k,\text{MLE}} = \mathbb{E}_{\boldsymbol{\nu}, \boldsymbol{\tau}} \left\{ \zeta(\boldsymbol{\nu}, \boldsymbol{\tau}) \tau_k \right\} \text{ and } \hat{\nu}_{k,\text{MLE}} = \mathbb{E}_{\boldsymbol{\nu}, \boldsymbol{\tau}} \left\{ \zeta(\boldsymbol{\nu}, \boldsymbol{\tau}) \nu_k \right\}, \quad (17)$$

in which $\zeta(\boldsymbol{\nu}, \boldsymbol{\tau})$ is defined as the following ratio:

$$\zeta(\boldsymbol{\nu}, \boldsymbol{\tau}) \triangleq \frac{\bar{\mathcal{L}}_c(\boldsymbol{\nu}, \boldsymbol{\tau})}{\bar{\mathcal{G}}(\boldsymbol{\nu}, \boldsymbol{\tau})}. \quad (18)$$

By using the new pseudo-pdf $\bar{\mathcal{G}}(\boldsymbol{\nu}, \boldsymbol{\tau})$, the expectations in (17) can be approximated as follows:

$$\hat{\tau}_{k,\text{MLE}} = \frac{1}{R} \sum_{r=1}^R \zeta(\boldsymbol{\nu}^{(r)}, \boldsymbol{\tau}^{(r)}) \tau_k^{(r)}, \quad (19)$$

$$\hat{\nu}_{k,\text{MLE}} = \frac{1}{R} \sum_{r=1}^R \zeta(\boldsymbol{\nu}^{(r)}, \boldsymbol{\tau}^{(r)}) \nu_k^{(r)}. \quad (20)$$

B. Choice of the Importance Function $\bar{\mathcal{G}}(\boldsymbol{\nu}, \boldsymbol{\tau})$

By closely inspecting the CLF, $\mathcal{L}_c(\boldsymbol{\nu}, \boldsymbol{\tau})$, one can notice that it is the matrix inverse, $(\mathbf{D}^H \mathbf{D})^{-1}$, that makes variable generation extremely tedious using the original normalized CLF. Fortunately, we will show in the sequel that a diagonal matrix is a valid approximation for $(\mathbf{D}^H \mathbf{D})$. First, the (k, k') th entry of $(\mathbf{D}^H \mathbf{D})$ is given by:

$$[\mathbf{D}^H \mathbf{D}]_{k,k'} = \sum_{m=1}^L \mathbf{d}_k[m]^* \mathbf{d}_{k'}[m], \quad (21)$$

with $\mathbf{d}_k[m]$ being the m^{th} element of the column vector $\mathbf{d}_k = \boldsymbol{\Lambda}(\nu_k) \mathbf{G}(\tau_k) \mathbf{t}_k$. Replacing $\boldsymbol{\Lambda}(\nu_k)$ and $\mathbf{G}(\tau_k)$ from (5) and (4) with their actual expressions leads to:

$$\mathbf{d}_k[m] = e^{j2\pi\nu_k(m-1)} \sum_{l=1}^L g([m-1]T_s - [l-1]T - \tau_k) \mathbf{t}_k[l]. \quad (22)$$

Now, by injecting (22) back into (21), it follows that:

$$\begin{aligned} [\mathbf{D}^H \mathbf{D}]_{k,k'} &= \sum_{m=1}^{QL} \left[\left(e^{-j2\pi\nu_k[m-1]} \sum_{l=1}^L g^*([m-1]T_s - [l-1]T - \tau_k) \mathbf{t}_k[l]^* \right) \right. \\ &\quad \left. \times \left(e^{j2\pi\nu_{k'}[m-1]} \sum_{l'=1}^L g([m-1]T_s - [l'-1]T - \tau_{k'}) \mathbf{t}_{k'}[l'] \right) \right]. \end{aligned}$$

The latter expression can be rewritten as:

$$[\mathbf{D}^H \mathbf{D}]_{k,k'} = \sum_{m=1}^{QL} \alpha_{\tau_k, \tau_{k'}}[m] e^{j2\pi(\nu_{k'} - \nu_k)[m-1]}, \quad (23)$$

with the coefficient $\alpha_{\tau_k, \tau_{k'}}[m]$ being defined as:

$$\begin{aligned} \alpha_{\tau_k, \tau_{k'}}[m] &= \sum_{l=1}^L \sum_{l'=1}^L \mathbf{t}_k[l]^* \mathbf{t}_{k'}[l'] g^*([m-1]T_s - [l-1]T - \tau_k) \\ &\quad \times g([m-1]T_s - [l'-1]T - \tau_{k'}). \end{aligned} \quad (24)$$

The diagonal elements of $\mathbf{D}^H \mathbf{D}$, i.e., $[\mathbf{D}^H \mathbf{D}]_{k,k}$, are simply obtained as:

$$[\mathbf{D}^H \mathbf{D}]_{k,k} = \sum_{m=1}^{QL} \alpha_{\tau_k, \tau_k}[m], \quad \text{for } k = 1, 2, \dots, K, \quad (25)$$

thereby leading to:

$$[\mathbf{D}^H \mathbf{D}]_{k,k} = \sum_{m=1}^{QL} \mathbf{t}_k^H \mathbf{g}_m(\tau_k)^H \mathbf{g}_m(\tau_k) \mathbf{t}_k. \quad (26)$$

Here $\mathbf{g}_m(\tau_k)$ is the m^{th} row of the matrix $\mathbf{G}(\tau)$. Moreover, it is worth noting that $\mathbf{g}_m(\tau_k)^H \mathbf{g}_m(\tau_k)$ is the same for all the possible values of τ_k , i.e., $\mathbf{g}_m(\tau_k)^H \mathbf{g}_m(\tau_k) = \mathbf{g}_m(0)^H \mathbf{g}_m(0)$, thereby yielding:

$$\begin{aligned} [\mathbf{D}^H \mathbf{D}]_{k,k} &= \sum_{m=1}^{QL} \mathbf{t}_k^H \mathbf{g}_m(0)^H \mathbf{g}_m(0) \mathbf{t}_k, \\ &= \mathbf{t}_k^H \mathbf{G}(0)^H \mathbf{G}(0) \mathbf{t}_k = \|\mathbf{G}(0) \mathbf{t}_k\|^2. \end{aligned} \quad (27)$$

We further assume, without loss of generality, that the K relays have the same transmission power, i.e., $\|\mathbf{G}(0) \mathbf{t}_k\|^2 = E_s$. Subsequently, the K diagonal elements have the same following expression:

$$[\mathbf{D}^H \mathbf{D}]_{k,k} = E_s, \quad \text{for } k = 1, 2, \dots, K. \quad (28)$$

Now, coming back to (23), one can notice the destructive superposition (for $k \neq k'$) of the complex exponentials¹ and the delayed RRC functions $[g(t - \tau_k)]$ and $[g(t - \tau_{k'})]$. Consequently, the off-diagonal elements of $\mathbf{D}^H \mathbf{D}$ are expected to be negligible compared to the diagonal entries of the same matrix. It follows that $\mathbf{D}^H \mathbf{D}$ can be accurately approximated by the following diagonal matrix :

$$\mathbf{D}^H \mathbf{D} \approx E_s \mathbf{I}_K. \quad (29)$$

This approximation can be validated empirically. Indeed, we first define the ratio between the off-diagonal and diagonal entries of $\mathbf{D}^H \mathbf{D}$ as follows:

$$\beta_{l,k} \triangleq \frac{\sum_{m=1}^{QL} \alpha_{\tau_k, \tau_{k'}}[m] e^{j2\pi(\nu_{k'} - \nu_k)[m-1]}}{\|\mathbf{G}(0) \mathbf{t}_k\|^2}. \quad (30)$$

¹This is reminiscent of multipath fading in wireless channels.

Then, we plot the complementary cumulative distribution function (CCDF) of $|\beta_{l,k}|$, i.e., $F_c(x) = Pr[|\beta_{l,k}| \geq x]$, by generating a large number of couples (τ_l, τ_k) and (ν_l, ν_k) . Those realizations are uniformly distributed in $[0, \tau_{\max}]^2$ and $[0, \nu_{\max}]^2$, respectively.

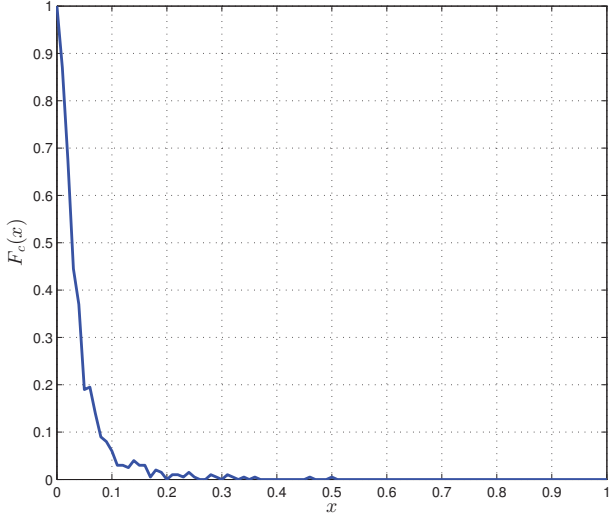


Fig. 1: CCDF of the magnitude of the ratio between the off-diagonal and diagonal entries of the matrix $\mathbf{D}^H \mathbf{D}$.

The result shown in Fig. 1 corroborates the approximation in (29). Indeed, the off-diagonal elements of $\mathbf{D}^H \mathbf{D}$ can be reasonably neglected as $|\beta_{l,k}|$ has almost-zero probability to exceed 0.15 for all $l \neq k$. Now, by using this approximation in (7), we obtain the following approximate CLF:

$$\mathcal{G}(\boldsymbol{\nu}, \boldsymbol{\tau}) = \frac{1}{E_s} \mathbf{x}^H \mathbf{D} \mathbf{D}^H \mathbf{x} = \frac{1}{E_s} \|\mathbf{D}^H \mathbf{x}\|^2, \quad (31)$$

which can be rewritten as follows:

$$\mathcal{G}(\boldsymbol{\nu}, \boldsymbol{\tau}) = \frac{1}{E_s} \sum_{k=1}^K |\mathbf{d}_k^H \mathbf{x}|^2 = \frac{1}{E_s} \sum_{k=1}^K \left| \sum_{m=1}^{QL} \mathbf{d}_k^*[m] \mathbf{x}[m] \right|^2. \quad (32)$$

By injecting the exact expression of $\mathbf{d}_k[m]$ into (32), the approximate CLF develops into:

$$\mathcal{G}(\boldsymbol{\nu}, \boldsymbol{\tau}) = \frac{1}{E_s} \sum_{k=1}^K I_k(\nu_k, \tau_k), \quad (33)$$

with $I_k(\nu, \tau)$ being the periodogram of the signal received from the k^{th} relay:

$$I_k(\nu, \tau) = \left| \sum_{l=1}^L \mathbf{t}_k[l] \left(\sum_{m=1}^{QL} x^*[m] e^{j2\pi\nu(m-1)} \times g([m-1]T_s - [l-1]T - \tau) \right) \right|^2. \quad (34)$$

The approximate CLF is the superposition of the individual relays' contributions. The corresponding pseudo-pdf is given by:

$$\bar{\mathcal{G}}(\boldsymbol{\nu}, \boldsymbol{\tau}) = \frac{\exp \left\{ \rho_1 \sum_{k=1}^K I_k(\nu_k, \tau_k) \right\}}{\int \cdots \int \exp \left\{ \rho_1 \sum_{k=1}^K I_k(\nu'_k, \tau'_k) \right\} d\nu' d\tau'}, \quad (35)$$

where ρ_1 is another design parameter to be chosen properly. Owing to the new approximation, which allows the separation of the contribution of each delay-CFO pair, it can be easily shown that the pseudo-pdf in (35) factorizes as follows:

$$\bar{\mathcal{G}}(\boldsymbol{\nu}, \boldsymbol{\tau}) = \prod_{k=1}^K \bar{g}_{\nu, \tau}^{(k)}(\nu_k, \tau_k), \quad (36)$$

where

$$\bar{g}_{\nu, \tau}^{(k)}(\nu, \tau) = \frac{e^{\rho_1 I_k(\nu, \tau)}}{\iint e^{\rho_1 I_k(\nu', \tau')} d\nu' d\tau'}. \quad (37)$$

It is worth mentioning here that the designed importance function, $\bar{\mathcal{G}}(\boldsymbol{\nu}, \boldsymbol{\tau})$, renders the generation process a lot easier. Indeed, instead of generating $\boldsymbol{\nu}^{(r)}$ and $\boldsymbol{\tau}^{(r)}$ using the original multidimensional distribution, one can easily generate, independently, K couples of realizations $(\nu_k^{(r)}, \tau_k^{(r)})$ with the bivariate distributions $\{\bar{g}_{\nu, \tau}^{(k)}(\nu, \tau)\}_{k=1}^K$, then construct the desired vector realizations as:

$$\boldsymbol{\nu}^{(r)} = [\nu_1^{(r)}, \nu_2^{(r)}, \dots, \nu_K^{(r)}]^T, \quad (38)$$

$$\boldsymbol{\tau}^{(r)} = [\tau_1^{(r)}, \tau_2^{(r)}, \dots, \tau_K^{(r)}]^T. \quad (39)$$

C. Estimations of the TDs and CFOs:

Once the required realizations are generated, the ML estimates can be obtained by using the *linear* sample mean, already presented in (19) and (20). An alternative way, allowing to alleviate the estimator bias (that may occur at very low SNR thresholds), is the use of the *circular* mean as follows:

$$\hat{\tau}_q = \tau_{\max} \left(\frac{1}{2\pi} \angle \left[\sum_{r=1}^R \zeta(\boldsymbol{\nu}^{(r)}, \boldsymbol{\tau}^{(r)}) \exp \left\{ j2\pi \left(\frac{\tau_k^{(r)}}{\tau_{\max}} - \frac{1}{2} \right) \right\} \right] + \frac{1}{2} \right), \quad (40)$$

$$\hat{\nu}_q = \nu_{\max} \left(\frac{1}{2\pi} \angle \left[\sum_{r=1}^R \zeta(\boldsymbol{\nu}^{(r)}, \boldsymbol{\tau}^{(r)}) \exp \left\{ j2\pi \left(\frac{\nu_k^{(r)}}{\nu_{\max}} - \frac{1}{2} \right) \right\} \right] + \frac{1}{2} \right), \quad (41)$$

where $\angle\{\cdot\}$ returns the argument of any complex number and $\zeta(\boldsymbol{\nu}^{(r)}, \boldsymbol{\tau}^{(r)})$ is the weighting coefficient defined in (18). By recalling the expression of the approximate pseudo-CLF, $\bar{\mathcal{G}}(\boldsymbol{\nu}, \boldsymbol{\tau})$, the weighting coefficient, $\zeta(\boldsymbol{\nu}^{(r)}, \boldsymbol{\tau}^{(r)})$, can be explicitly expressed as follows:

$$\zeta(\boldsymbol{\nu}^{(r)}, \boldsymbol{\tau}^{(r)}) = \frac{\int \cdots \int \exp \left\{ \rho_1 \sum_{k=1}^K I_k(\nu_k, \tau_k) \right\} d\nu d\tau}{\int \cdots \int \exp \{ \rho_0 \mathcal{L}_c(\boldsymbol{\nu}, \boldsymbol{\tau}) \} d\nu d\tau} \times \exp \left\{ \rho_0 \mathcal{L}_c(\boldsymbol{\nu}^{(r)}, \boldsymbol{\tau}^{(r)}) - \rho_1 \sum_{k=1}^K I_k(\nu_k^{(r)}, \tau_k^{(r)}) \right\}. \quad (42)$$

We provide two hints to reduce the computational complexity related to the evaluation of this coefficient. First, being real and positive, the integrals ratio in (42) can be dropped since only the argument of the complex quantities is needed in (40) and (41) to estimate the delay and CFOs. Second, a computational overflow may occur while evaluating the weighting coefficient, especially with a large value of ρ_0 [which is indeed required to satisfy the

constraint in (12)]. Consequently, we use the following *normalized* weighting coefficient without any changes in the final results:

$$\bar{\zeta}(\boldsymbol{\nu}^{(r)}, \boldsymbol{\tau}^{(r)}) = \exp \left\{ \rho_0 \mathcal{L}_c(\boldsymbol{\nu}^{(r)}, \boldsymbol{\tau}^{(r)}) - \rho_1 \sum_{k=1}^K I_k(\nu_k^{(r)}, \tau_k^{(r)}) - \max_{1 \leq r \leq R} \left[\rho_0 \mathcal{L}_c(\boldsymbol{\nu}^{(r)}, \boldsymbol{\tau}^{(r)}) - \rho_1 \sum_{k=1}^K I_k(\nu_k^{(r)}, \tau_k^{(r)}) \right] \right\}. \quad (43)$$

V. SIMULATION RESULTS

In this section, we assess the performance results of the new IS-based ML estimator in terms of the mean square error (MSE) with a total number of Monte-Carlo runs $M_c = 1000$. In our simulation, we consider a DF system composed of one source, one destination and $K = 2$ relay nodes. The training sequence consists of 32 symbols taken from a 16-QAM constellation. The pulse shaping function is a SRRC with a roll-off factor $\alpha = 0.3$. The design parameter, ρ_1 , is set to 15, and ρ_0 , which must be sufficiently high, is set to 8000. It was also found that $R = 1000$ generated realizations provide sufficiently accurate MLEs for both the MTOs and CFOs.

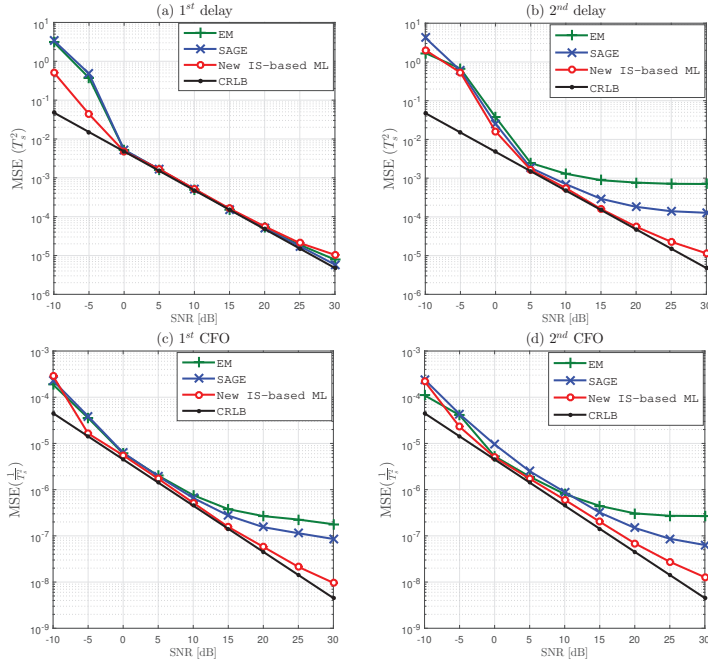


Fig. 2: MSE for MTOs and CFOs joint estimation with $L = 32$ symbols, $Q = 2$, $\alpha = 0.3$, $K = 2$, and 16-QAM.

Fig. 2 depicts the MSE of the proposed joint ML estimator and the two iterative algorithms (i.e., expectation-maximization and space-alternating generalized expectation-maximization) presented in [15]. We also plot the Cramer-Rao lower bound (CRLB) as an overall benchmark for the best performance achievable in theory. The new IS-based approach is able to estimate all the synchronization parameters with very high accuracy. Moreover, it achieves the CRLB over a wide range of practical SNRs thereby validating its statistical efficiency in practice. Moreover, it outperforms the two iterative algorithms of [15] for medium to high SNR levels. Indeed, contrarily to the proposed IS-based solution, the ML algorithms of [15] suffer from lack of global convergence as they are iterative in nature.

VI. CONCLUSION

In this paper, we proposed a new joint multiple time and carrier frequency offsets ML estimator that leverages the powerful importance sampling concept. The new estimator always achieves the global maximum of the likelihood function. Simulation results illustrate unambiguously the clear superiority of the new IS-based ML estimator over iterative state-of-the-art techniques without resorting, however, to a non-iterative grid search.

REFERENCES

- [1] X. Li, C. Xing, Y.-C. Wu, and S. C. Chan, "Timing estimation and resynchronization for amplify-and-forward communication systems," *IEEE Trans. Signal Process.*, vol. 58, no. 4, pp. 2218-2229, Apr. 2010.
- [2] H. Mehrpouyan and S. D. Blostein, "Estimation, training, and effect of timing offsets in distributed cooperative networks," in *Proc. IEEE Global Commun. Conf. (GLOBECOM)*, Miami, FL, Dec. 2010.
- [3] M. T. Hossain, D. B. Smith, and S. Kandeepan, "Timing synchronization for cooperative communications with detect and forward relaying," *Springer J. Wireless Pers. Commun.*, 2010.
- [4] X. Li, Y. C. Wu, and E. Serpedin, "Timing synchronization in decode-and-forward cooperative communication systems," *IEEE Trans. Signal Process.*, vol. 57, no. 4, pp. 1444-1455, Apr. 2009.
- [5] H. Mehrpouyan and S. D. Blostein, "Bounds and algorithms for multiple frequency offset estimation in cooperative networks," *IEEE Trans. Wireless Commun.*, vol. 10, no. 4, pp. 1300-1311, Apr. 2011.
- [6] O. Besson and P. Stoica, "On parameter estimation of MIMO flat-fading channels with frequency offsets," *IEEE Trans. Signal Process.*, vol. 51, no. 3, pp. 602-613, Mar. 2003.
- [7] T. Pham, A. Nallanathan, and Y. Liang, "Joint channel and frequency offset estimation in distributed MIMO flat-fading channels," *IEEE Trans. Wireless Commun.*, vol. 7, no. 2, pp. 648-656, Feb. 2008.
- [8] Y. Yao and T. Ng, "Correlation-based frequency offset estimation in MIMO system," in *Proc. IEEE Veh. Technol. Conf. (VTC)*, Orlando, FL, Oct. 2003.
- [9] Z. Lu, J. Li, L. Zhao, and J. Pang, "Iterative parameter estimation in MIMO flat-fading channels with frequency offsets," in *Proc IEEE Int. Conf. Advanced Inf. Netw. Appl. (AINA)*, Austria, Apr. 2006.
- [10] Y. Tian, X. Lei, Y. Xiao, and S. Li, "ML synchronization algorithm and estimation bounds for cooperative systems," in *Proc IEEE Pacific Asia Conf. on Circuits, Commun. and Systems (PACCS)*, China, Aug. 2010.
- [11] L. Dai, Z. Wang, J. Wang, and Z. Yang, "Joint channel estimation and time-frequency synchronization for uplink TDS-OFDMA systems," *IEEE Trans. Consumer Electron.*, vol. 56, no. 2, pp. 494-500, May 2010.
- [12] J.-H. Lee and S.-C. Kim, "Time and frequency synchronization for OFDMA uplink system using the SAGE algorithm," *IEEE Trans. Wireless Commun.*, vol. 6, no. 4, pp. 1176-1181, Apr. 2007.
- [13] M. Morelli, "Time and frequency synchronization for the uplink of an OFDMA system," *IEEE Trans. Commun.*, vol. 52, no. 2, pp. 296-396, Feb. 2004.
- [14] M.-O. Pun, M. Morelli, and C.-C. J. Kuo, "Maximum likelihood synchronization and channel estimation for OFDMA uplink transmissions," *IEEE Trans. Commun.*, vol. 54, no. 4, pp. 726-736, Apr. 2006.
- [15] A. A. Nasir, H. Mehrpouyan, S. Durani, R. A. Kennedy, and S. D. Blostein, "Timing and carrier synchronization with channel estimation in multi-relay cooperative networks," *IEEE Trans. Signal Process.*, vol. 60, no. 2, pp. 793-811, Feb. 2012.
- [16] H. Meyr, M. Moeneclaey, and S. A. Fechtel, *Digital Communication Receivers, Synchronization, Channel Estimation, and Signal Processing*, J. G. Proakis, Ed. Wiley Series in Telecommunications and Signal Processing, 1998.
- [17] M. Pincus "A closed form solution for certain programming problems", *Oper. Res.*, pp. 690-694, 1962.